Asian Journal of Chemistry; Vol. 33, No. 12 (2021), 2953-2964

ASIAN JOURNAL OF CHEMISTRY

https://doi.org/10.14233/ajchem.2021.23394

Corrosion Inhibitive Properties of 5-(4-Aminophenyl)-1,3,4-oxadiazole-2-thiol and 5-(4-Methylphenyl)-1,3,4-oxadiazole-2-thiol on Mild Steel in 1.0 M HCl Solution

VIKAS KALIA, PRADEEP KUMAR, SURESH KUMAR and HARIOM DAHIYA*

Department of Chemistry, Maharshi Dayanand University, Rohtak-124001, India

*Corresponding author: E-mail: harichem2007@gmail.com

Received: 30 June 2021; *Accepted*: 25 August 2021; *Published online*: 6 December 2021; AJC-20585

The corrosion inhibition consequence of 5-(4-aminophenyl)-1,3,4-oxadiazole-2-thiol (APOT) and 5-(4-methylphenyl)-1,3,4-oxadiazole-2-thiol (MPOT) were accomplished by employing weight loss measurement, electrochemical impedance spectroscopy (EIS), potentiodynamic polarization measurement and scanning electron microscope (SEM). An impact of immersion time 12.0 h and different temperatures (298, 308 and 318 K) with solution of 1.0 M HCl, which include various concentration of inhibitor at the corrosion of mild steel were designed. Weight loss measurement showed that with enhancing the concentration of these studied inhibitors the percentage inhibition efficiency (IE%) enhances, but corrosion rate (CR) diminishes while reverse condition in case of temperatures change. The electrochemical impedance spectroscopy examine pointed out that the charge transfer resistance (R_{ct}) values enhances and consequently the double layer capacitance (C_{dl}) values diminishes with rising each inhibitor concentration in 1.0 M HCl and also there is a formation of adsorption coating at the metal surface. Polarization measurement showed that both APOT and MPOT perform as mixed type corrosion inhibitors. Furthermore, the adsorption behaviour on surface of mild steel for each studied inhibitor results the Langmuir adsorption isotherm. Surface conduct of mild steel also designed through the SEM and energy dispersive X-ray (EDX) analysis and concludes that there is evolution of inhibitive film of APOT and MPOT on the surface of mild steel.

Keywords: Oxadiazole derivatives, Mild steel, Inhibitor, HCl, EIS, Polarization.

INTRODUCTION

Acid solutions are typically utilized in a wide range of industrial process like acid purification, acid pickling, oil-well acidification and acid removing [1-5]. Specifically, hydrochloric acid and sulfuric acid are associated with metal cleaning to eliminate rust and unwanted mill scale. Hence, aggressive acidic solution corrodes the metal surface and causes the deterioration of metallic structure. Mild steel is usually employed in various industrials and engineering fields because of its incredible mechanical properties and minimal cost and simple accessibility, however most disadvantage of mild steel is that it is highly sensible to corrosion attack and it's also dissolute in acidic medium [5,6]. Different strategies are adopted to secure the surface of metal against corrosion assault. However, the use of corrosion inhibitors were found to be the more effective application for blockage the corrosion of metals in the acidic environment [7-9]. Among numerous types of corrosion inhi-bitors, the synthesized organic compounds as corrosion inhibitor are found to be very efficient approach to deal with secure metal surface.

The choice of organic inhibitors over inorganic inhibitor as a result of it incorporates electronegative group, π electron in multiple bonds and aromatic ring in structure form; these act as fundamental adsorption facilities [10-12]. From literature, it is found that the organic compound that containing electronegative groups, aromatics rings and heteroatom's like N, O and S are recognized to be the productive corrosion inhibitor [13,14]. The adsorption action on the metal surface of organic compounds additionally relies on the molecular structure, size, weight and nature of substituent, steric components and electron density present on the donor atom [15,16]. The fundamental role of organic corrosion inhibitors is that when very low concentration added to corroding medium, it diminishes the dissolution rates of metals and hindered the corrosion by adsorption procedure on the metal surface [17-19]. Further, these

inhibitor molecules formed a bond with the metal surface through donating the electron lone pair and/or electron present at the donor atom of inhibitors hence reduces the corrosion rates in acidic medium. Subsequently, these inhibitors inhibit the metal by developing the protective layer at surface of metal and address great inhibitive properties.

The oxadiazole compounds recommend an appropriate potential to impede corrosion of metals in acidic environment [20,21]. Oxadiazole derivatives rich in heteroatom's (N, O and S), by which these derivatives possess good adsorption process on the metal surface and furthermore saw as ecological familiar inhibitors because of their attributes of extreme chemical activities and minor harmful in nature [22]. Recently, numerous authors work on the evolution of new corrosion inhibitors like pyrazole [23,24], triazole [25,26], tetrazole [27,28], imidazole [29] and oxadiazole derivatives [30,31]. The choice of oxadiazole derivatives with numerous substituents as a corrosion inhibitor is depend upon the presence heteroatoms like nitrogen, sulfur and oxygen in aromatic system, which encourages electrophilic assault [32,33].

In present work, the corrosive inhibitive properties of 5-(4-aminophenyl)-1,3,4-oxadiazole-2-thiol (APOT) and 5-(4-methylphenyl)-1,3,4-oxadiazole-2-thiol (MPOT) on corrosion of mild steel in 1.0 M HCl for immersion period of 12 h at 298, 308 and 318 K were examined. The corrosion analyses were accomplished through different methods *i.e.* weight loss exami-nation, electrochemical impedance and potentiodynamic polari-zation. Similarly, to recognize adsorption behaviour of utilized inhibitors at the surface of mild steel, a Langmuir adsorption isotherm and some thermodynamic parameters have also been examined.

EXPERIMENTAL

The corrosion inhibition was accomplished with mild steel of the subsequent composition (wt%): C = 0.054, Cr = 0.056, Mn = 0.26, Cu = 0.010, P = 0.019, Ti = 0.002, S = 0.017, Mo = 0.018, Si = 0.015, Ni = 0.009 and remained Fe. The samples cut into 3 cm × 1.5 cm pieces were used to weight loss experiment whereas samples of size 1 cm × 1 cm with 1 cm^2 uncovered surface region as working electrode were utilized for electrochemical examinations. Before start the analysis the mild steel samples surface were mechanically scraped with various grade emery papers up to 1000 grade. The samples were therefore cleaned with the double distilled water, degreased with the acetone, dry with hot air blower and afterward positioned in desiccators for test utilized.

Corrosion inhibitor: 5-(4-Aminophenyl)-1,3,4-oxadiazole-2-thiol (APOT) and 5-(4-methylphenyl)-1,3,4-oxadiazole-2-thiol (MPOT) (Fig. 1) both purchased from Sigma-Aldrich (97%) were employed as corrosion inhibitors. The molecular formula and molecular mass of APOT is $C_8H_7N_3OS$ and 193.23 g/mol and MPOT is $C_9H_8N_2OS$ and 192.24 g/mol, respectively.

Preparation of solutions: The test arrangement of 1.0 M HCl solution was set up through dilution of AR grade 37% HCl along with the double distilled water. An ideal solution of each oxadiazole derivatives is managed in a ratio of 10:1 in water and ethanol combination by volume; to formed solubility

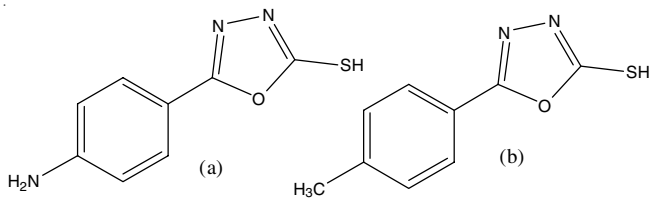

Fig. 1. Structure of (a) 5-(4-aminophenyl)-1,3,4-oxadiazole-2-thiol (b) 5-(4-methylphenyl)-1,3,4-oxadiazole-2-thiol

through applying 1.0 M HCl. All corrosion experiments were carried out in 1.0 M HCl solution without and with the numerous concentrations (50-300 ppm) of each corrosion inhibitors.

Weight loss measurement: Weight reduction assessments have been completed in wooden air thermostat. After balancing the mild steel specimens, immersed in 50 mL beaker of analysis solution, which consists of 1.0 M HCl with numerous concentrations of corrosion inhibitor at different temperatures for 12 h immersion periods. Subsequently, the finishing of required immersion period, the specimens were removed, cleaned carefully with double distilled water, degreased with the acetone, dried and further weighed accurately. Triplicate weight loss measurements have been conducted for each temperatures and time periods. Then, the average weight decrease values have been taken to determine the different corrosion parameters. The corrosion rate (CR%) was determined using eqn. 1:

$$CR\ (mm\ y^{-1}) = \frac{87.6 \times W}{A \times t \times D} \quad (1)$$

where, w is the weight reduction of mild steel in mg, A is an area of specimen (cm^2), t is an exposure time (h) and D is the density of mild steel (g cm^{-3}).

The surface coverage (θ) and percentage corrosion inhibition efficiency (η_w%) were estimated through eqns. 2 and 3:

$$\theta = \frac{w_o - w_i}{w_o} \quad (2)$$

$$\eta\ (\%) = \frac{w_o - w_i}{w_o} \times 100 \quad (3)$$

where, w_o and w_i are the weight reduction of mild steel in absence and presence of numerous concentrations of inhibitor compounds, respectively.

Electrochemical measurements: Three electrode cell assemblies were adopted to record the electrochemical conduct of mild steel in 1.0 M HCl solution with existence of numerous concentration of corrosion inhibitor. The three cell electrode including platinum mesh as counter electrode (CE), saturated calomel electrode (SCE) as the reference electrode (RE) and mild steel specimens with uncovered surface area 1.0 cm × 1.0 cm as working electrode and remaining area covered with epoxy resin. Both electrochemical impedance and potentiodynamic polarization estimations have been performed using Princeton Applied Research parastat-4000. Before start analysis the electrode have been immersed in to 250 mL experimental solution beaker at open circuit potential (OCP) 30 min at room temperature to be enough to attain as stable value of OCP.

Electrochemical impedance spectroscopy (EIS): The electrochemical impedance spectroscopy assessments have

been done at the corrosion potential ($-E_{corr}$) at frequency value of 10 kHz to 0.01 Hz with a signal amplitude of 10 mV with AC signal. Whole impedance estimations have been consequently controlled through Z-view software. The main impedance criterions like charge transfer resistance (R_{ct}) and the double layer capacitance (C_{dl}) have been considered from analyze the EIS diagram.

Potentiodynamic polarization: The polarization evaluation has been performed subsequently the EIS measurement. During polarization investigation, anodic and cathodic potentiodynamic polarization Tafel curves have been reported by altering the potential value from -250 mV to +250 mV in order to open circuit potential, at a scan rate of 1.0 mV/s. Additionally, the corrosion current density (I_{corr}) value was acquired through extrapolating linear segment of anodic and cathodic Tafel plots. Through polarization measurement, the corrosion parameters like corrosion potential ($-E_{corr}$), corrosion current density (I_{corr}), cathodic (β_c) and anodic (β_a) Tafel constant have been acquired.

SEM-EDX analysis: The SEM techniques have been carried out to examine the surface conduct of mild steel samples, which were immersed in to blank solution and solution that contain 300 ppm concentration of both corrosion inhibitors for 12 h at 298, 308, 318 K, respectively using SEM-EDX (ZEISS) scanning electronic microscope.

RESULTS AND DISCUSSION

Weight loss determination: To check the corrosion rate and inhibitive effect of APOT and MPOT on the mild steel surface the weight reduction experimentation is one of the most positive approaches due to its simple exercise, application and reliability [34]. This technique is extensively adopted by most of researchers [35-38]. In current investigation, APOT and MPOT have been analyzed as corrosion inhibitors on mild steel in 1.0 M HCl for an immersion periods of 12 h at 298, 308, 318 K.

Effect of concentration: Fig. 2a-b shows the corrosion rate plots and Fig. 3a-b concerned for the corrosion inhibition efficiency curves of both studied corrosion inhibitor. The value of the corrosion rate (CR) diminishes and corrosion inhibition efficiency ($\eta_{w\%}$) enhances on increasing the inhibitors concentration and reaches higher value which is specific for both the inhibitors. This behaviour might be ascribed to the evidence that at the higher concentration of corrosion inhibitor, the adsorption phenomena may go through the large capability level above the metal surface. From current investigation, for APOT the maximum inhibition efficiency were increased up to 80.82% and 71.91% for MPOT, respectively just at a significant lower concentration of 300 ppm for both derivatives.

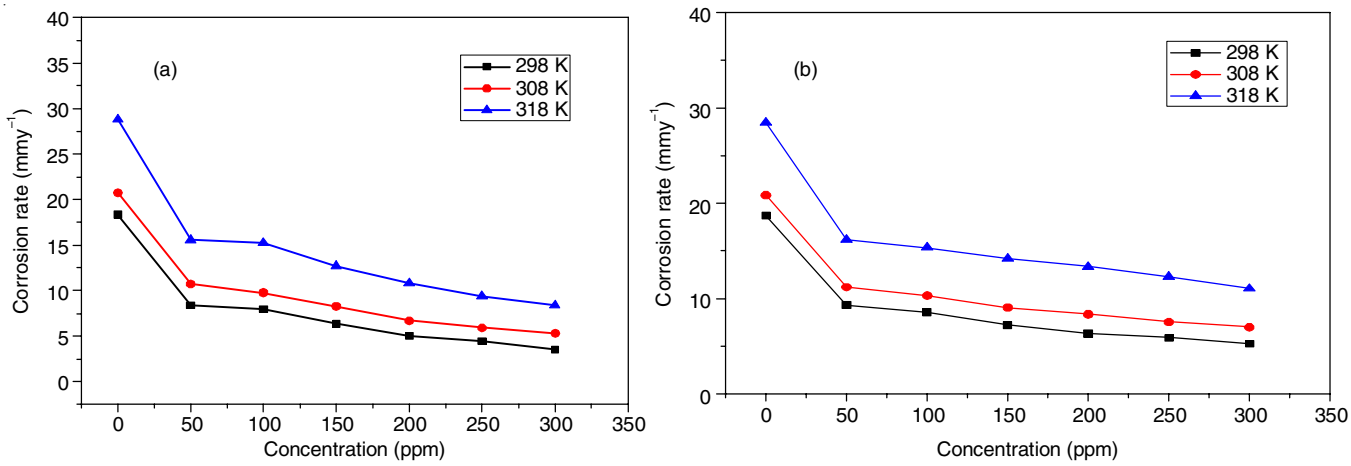

Fig. 2. Alteration of corrosion rates (CR) with different concentrations of APOT and MPOT at 298, 308 and 318 K for an immersion periods of 12 h

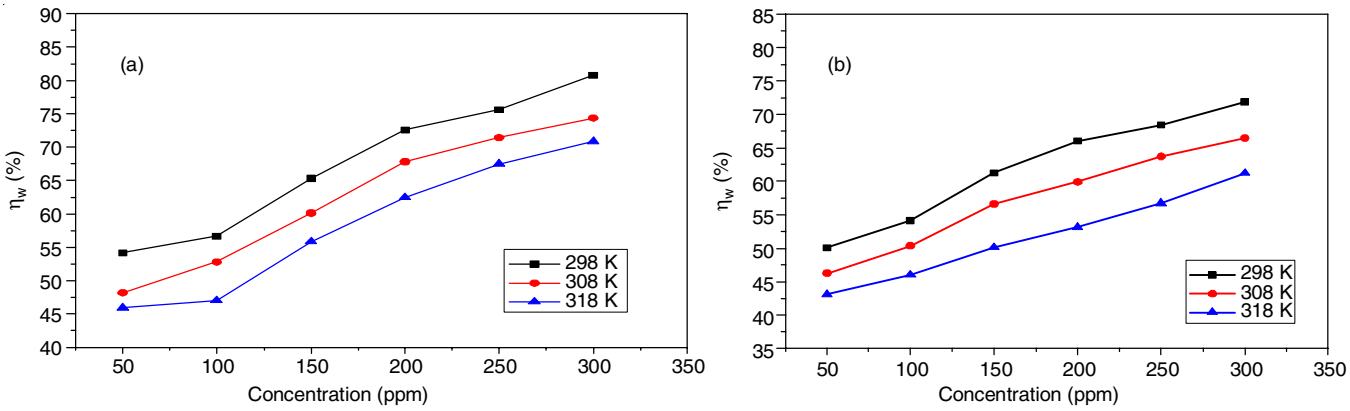

Fig. 3. Alteration of corrosion inhibition efficiency ($\eta_{w\%}$) with different concentration of APOT and MPOT at 298, 308 and 318 K for an immersion periods of 12 h

Various calculated experimental values from weight loss data *i.e.* corrosion inhibition efficiency, surface coverage and corrosion rate without and with numerous concentration of APOT and MPOT inhibitors in 1.0 M HCl solution for immersion periods of 12 h at varying temperatures range are shown in Table-1, which shows that an inhibition efficiency of mild steel enhances but the corrosion rate diminishes with increasing the concentrations from 50 to 300 ppm for both studied corrosion inhibitors. Both inhibitors are responsible due to its enhanced adsorption on the mild steel surface [39], which protects the surface perfectly from the corrosive environment.

TABLE-1
CALCULATED DATA OF WEIGHT REDUCTION MEASUREMENT FOR CORROSION OF MS IN 1.0 M HCl SOLUTION IN THE EXISTENCE OF NUMEROUS CONCENTRATIONS OF APOT AND MPOT FOR IMMERSION PERIODS 12 h AT 298, 308 AND 318 K

Temp. (K)	Conc. (ppm)	APOT			MPOT		
		CR (mm y^{-1})	η_w (%)	θ	CR (mm y^{-1})	η_w (%)	θ
298	0	18.34	–	–	18.72	–	–
	50	08.39	54.23	0.54	09.34	50.08	0.50
	100	07.95	56.64	0.56	08.58	54.14	0.54
	150	06.36	65.28	0.65	07.25	61.25	0.61
	200	05.03	72.53	0.72	06.36	65.98	0.65
	250	04.46	75.64	0.75	05.92	68.35	0.68
	300	03.51	80.82	0.80	05.26	71.91	0.71
308	0	20.75	–	–	20.88	–	–
	50	10.74	48.24	0.48	11.21	46.28	0.46
	100	09.79	52.82	0.52	10.36	50.37	0.50
	150	08.27	60.15	0.60	09.06	56.60	0.56
	200	06.68	67.78	0.67	08.36	59.93	0.59
	250	05.92	71.45	0.71	07.57	63.73	0.63
	300	05.32	74.35	0.74	07.00	66.46	0.66
318	0	28.80	–	–	28.48	–	–
	50	15.55	45.98	0.45	16.19	43.15	0.43
	100	15.24	47.08	0.47	15.36	46.05	0.46
	150	12.70	55.88	0.55	14.19	50.16	0.50
	200	10.80	62.48	0.62	13.33	53.17	0.53
	250	09.37	67.43	0.67	12.32	56.72	0.56
	300	08.39	70.84	0.70	11.05	61.17	0.61

Effect of temperature: The impact of temperatures on the corrosion inhibitive characteristics of different concentration of both inhibitors on mild steel in 1.0 M HCl solution about temperature range of 298 to 318 K was investigated. It was concluded that with increasing the temperature from 298 to 318 K, the weight loss of mild steel enhanced therefore the value of corrosion rates also enhanced but an inhibition efficiency value diminished at similar concentration of both inhibitors.

Hence, the increased in corrosion rate values with rise in temperature might be as a result of quick desorption and disintegration and/or displacement of inhibitor compounds [40], which results in decreased in the intensity of adsoption process on the mild steel surface. Oguzie *et al.* [41] recommends that the reduction in inhibition efficiency with increasing temperature shows the inhibitor compounds exist through physically adsorbed on to the surface of metal, although an opposite action indicates the compounds absorbed on surface by the process of chemisorptions. Hence, the adsorption action of APOT and MPOT are generally due to the physical adsorption process. Moreover, the rise in temperature mostly accelerates the hydrogen evolution reaction, which causes a higher destruction rate of the mild steel.

Thermodynamic studies: Thermodynamic parameters *i.e.* activation energy, enthalpy and entropy give the additional observation about corrosion inhibition component, which was investigated from Arrhenius equation and transition state curve (eqns. 4 and 5) [42,43]:

$$\ln CR = A - \frac{E_a}{RT} \quad (4)$$

$$CR = \frac{RT}{Nh}\exp\left(\frac{\Delta S^{\#}}{R}\right)\exp\left(\frac{-\Delta H^{\#}}{RT}\right) \quad (5)$$

where, CR is the corrosion rate (mm y^{-1}), A is the Arrhenius pre-exponential factor for corrosion method, E_a is the energy of activation (kJ mol^{-1}), R is the molar gas constant (8.314 J K^{-1} mol^{-1}), T is the absolute temperature (Kelvin), h is the Plank's constant and N is the Avogadro's number. The Arrhenius curve between ln CR *vs.* 1000/T and transition state curve between ln (CR/T) and 1000/T for corrosion of mild steel in 1.0 M HCl without and with various concentrations of APOT and MPOT are shown in Figs. 4 and 5.

Table-2 represents the calculated value of the thermodynamic parameters like E_a, $\Delta H^{\#}$ and $\Delta S^{\#}$ which are acquired from the slope of ($-E_a/R$), ($-\Delta H^{\#}/T$) and intercept of ln (R/Nh) + $\Delta S^{\#}/R$ of Arrhenius and transition plots for mild steel in 1.0 M HCl with existence of numerous concentrations of both corrosion inhibitors.

TABLE-2
VARIOUS ACTIVATION CRITERIONS FOR MS IN 1.0 M HCl IN THE EXISTENCE OF NUMEROUS CONCENTRATIONS OF APOT AND MPOT AT VARYING TEMPERATURES FOR IMMERSION PERIOD 12 h

Conc. (ppm)	APOT			MPOT		
	E_a (kJ mol^{-1})	$\Delta H^{\#}$ (kJ mol^{-1})	$\Delta S^{\#}$ (J mol^{-1} K^{-1})	E_a (kJ mol^{-1})	$\Delta H^{\#}$ (kJ mol^{-1})	$\Delta S^{\#}$ (J mol^{-1} K^{-1})
Blank	25.18	20.89	-151.89	23.80	19.55	-156.20
50	24.29	21.73	-154.32	21.64	19.08	-162.44
100	26.52	23.99	-147.80	23.90	22.47	-152.21
150	27.20	23.28	-151.19	26.43	23.87	-148.51
200	30.05	27.49	-139.24	29.12	26.56	-140.53
250	30.09	26.65	-143.07	30.28	26.82	-140.37
300	34.27	31.71	-128.11	28.91	26.95	-141.00

The activation energy (E_a) have been determined to be high in the existence of concentration of both utilized inhibitors which imply the decreases in the corrosion action on mild steel in the presence of both APOT and MPOT inhibitors. The enhance in activation energy indicate that the adsorption of inhibitors compounds established an energy barrier against corrosion process, which appeared to decreased in corrosion rate [44]. Thus, it is suggested that the higher value of activation energy value in the inhibited solution support the physical

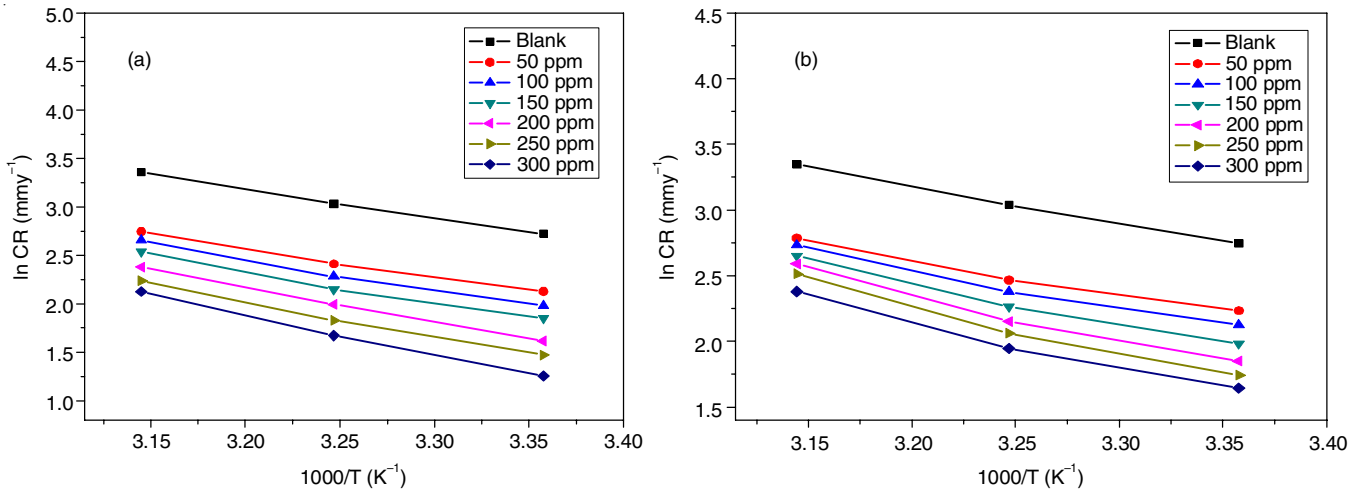

Fig. 4. Arrhenius curves of ln CR against 1000/T for corrosion of mild steel with numerous concentrations of APOT and MPOT in 1.0 M HCl at 298, 308 and 318 K for 12 h

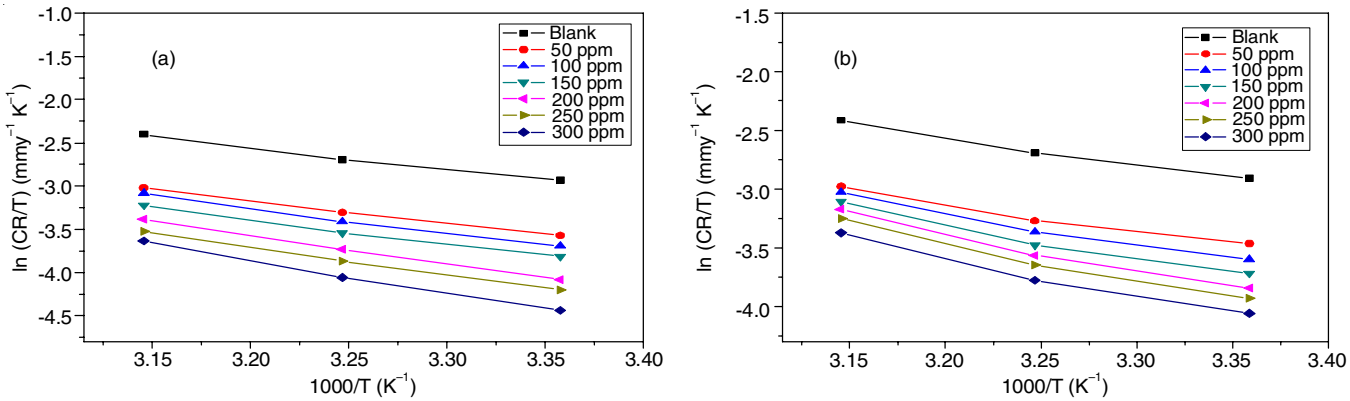

Fig. 5. Plots of ln (CR/T) *vs.* 1000/T for corrosion of mild steel with numerous concentrations of the APOT and MPOT in 1.0 M HCl at 298, 308 and 318 K for 12 h

adsorption (physisorption) phenomenon, whereas its show lower activation energy (E_a) for inhibited solution correlated to blank (1.0 M HCl) solution which signify a chemical adsorption (chemisorptions) phenomenon [45]. In current study, the value of E_a for both inhibited solution is higher as compared to blank solution indicating a physisorption phenomena for both corrosion inhibitors.

Furthermore, it was also concluded that value of enthalpy ($\Delta H^{\#}$) of activation is positive and enhance with enhancing concentration of both APOT and MPOT in 1.0 M HCl is endothermic in nature [46]. The estimation of entropy change ($\Delta S^{\#}$) with a negative sign at the activated positions for both used inhibitor compounds exhibits the development of activated complex which can occur through the association rather than the dissociation step. Hence suggested that as the transition from the reactant to an activated complex, there is a decrease in the disorder (randomness) [47].

Adsorption isotherms: The main factor for an organic compounds to be examined as corrosion inhibitors is its tedency to get adsorbed on surface of metal by blocking the active site and substituted the water molecules to form a inhibitive film on to metal surface to diminish the corrosion process [48]. The adsorption action mainly depends on various factors such as nature of metal, electronic and the steric components of an adsorbate, temperature range and different surface site [49]. In present investigations, various adosrption isotherms *i.e.* Frumkin, Langmuir isotherm, Temkin, Freundlich and Flory-Huggins have been proposed to determine the adsorption process. However among the studied isotherms, a straight line curve in the Langmuir adsorption isotherm was best fitted for the studied corrosion inhibitors. The plots of C_{inh}/θ *vs.* C_{inh} for immersion periods 12 h at 298, 308 and 318 K (Figs. 6 and 7) shows a straight line curve with a relatively unit correlation coefficient ($R^2 > 0.99$). Langmuir adsorption isotherm could be interpreted according to eqn. 6 [50].

$$\frac{C_{inh}}{\theta} = \frac{1}{K_{ads}} + C \qquad (6)$$

where, C_{inh} is the corrosion inhibitor concentration, θ and K_{ads} are the degree of surface coverage and an equilibrium constant of the adsorption process, respectively.

Furthermore, the value of K_{ads} which is measured by the reciprocal value of the intercept of the related straight plots in Langmuir isotherms, which was also used to calculate the standard free energy of adsorption ($\Delta G°_{ads}$) using eqn. 7 [51].

$$\Delta G^{o}_{ads} = -RT \ln(1\times10^{6} K_{ads}) \qquad (7)$$

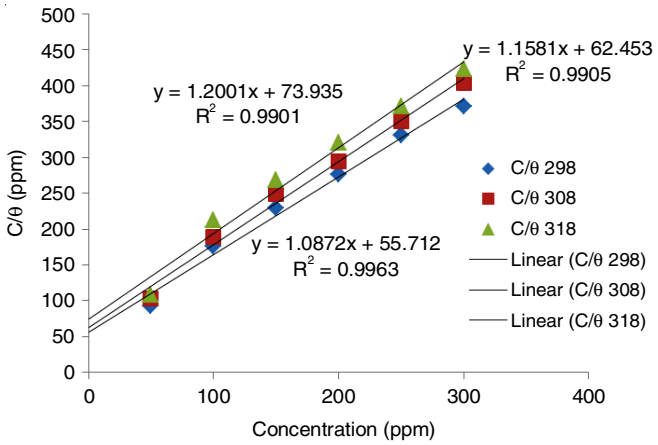

Fig. 6. Langmuir adsorption isotherm graphs for the mild steel in 1.0 M HCl with different concentrations of APOT at 298, 308 and 318 K for an immersion periods of 12 h

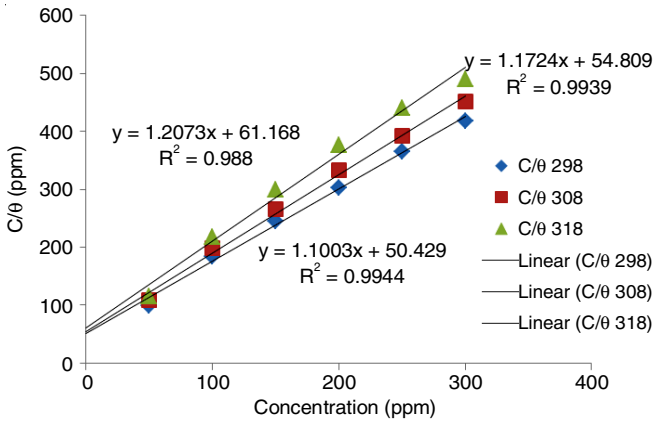

Fig. 7. The curve of Langmuir adsorption isotherm for the mild steel in 1.0 M HCl with numerous concentration of MPOT at 298, 308 and 318 K for an immersion periods of 12 h

where, R value denotes an universal gas constant (8.314 J mol^{-1} K^{-1}), 1×10^6 address the concentration of water (mg L^{-1}) and T is the absolute temperature (Kelvin).

The adsorption components such as K_{ads}, slope and ΔG°_{ads} values for both corrosion inhibitors are listed in Table-3, which concludes that with enhances in the temperature, the value of K_{ads} diminishes moderately, which confirms that at lower temperature the inhibitors strongly adsorbed on the metal surface. Hence, a great value of K_{ads} specifies the more active adsorption of corrosion inhibitors on to the surface of mild steel and also shows greater inhibition efficiency.

Additionally, a negative value of ΔG°_{ads} signifying the spontaneous behaviour of adsorption of inhibitor on metal surface [52]. Normally, the value of ΔG°_{ads} about -20 kJ mol^{-1} expresses the physical adsorption of corrosion inhibitors through the interaction *via* weak van der Waals forces in between charged inhibitor molecules and charged metal surface. A higher negative value -40 kJ mol^{-1} of ΔG°_{ads} indicates the chemical adsorption (chemisorptions), which is due to charge sharing or transfer from inhibitor molecule to surface of metal to form a coordinate type bond [53].

The determined ΔG°_{ads} values in present investigation were found to be -24.27 to -25.15 kJ mol^{-1} for APOT and -24.51 to -25.65 kJ mol^{-1} for MPOT for immersion periods of 12 h at 298 to 318 K that lies in between -20 and -40 kJ mol^{-1}, which confirmed that both inhibitors function as mixed type of adsorption with dominant nature of physical adsorption.

Electrochemical impedance spectroscopy analysis: The electrochemical application was accomplished for corrosion on mild steel surface in 1.0 M HCl with various concentrations for both inhibitors at 298 K. The Nyquist plot of corrosion of mild steel in 1.0 M HCl solution in absence and presence of different concentrations of APOT and MPOT at 298 K are shown in Fig. 8. The Nyquist diagram implies that impedance curves are single semicircle type, which implies that diameter of these semicircles enhances with enhancing the concentration of corrosion inhibitors in 1.0 M HCl. Moreover, also diameter of loop is not perfect semicircle and this deviation is assigned to the frequency dispersal of interfacial impedance that frequently associated to the roughness, homogeneities as well as adsorption activity of the corrosion inhibitor on to the metal surface [54-56].

The related impedance parameters for both inhibitors such as the value of charge transfer resistance (R_{ct}); the double layer capacitance (C_{dl}) and the percentage corrosion inhibition efficiency (η_{eis}%) are recorded in Table-4. It is observed that the value of charge transfer resistance R_{ct} enhances with increasing concentrations of each inhibitor which is due to the evolution of inhibitive layer on the mild steel solution interface [57]. Further, the charge transfer resistance (R_{ct}) value acquired the distinction in real impedance value at higher to lower frequency. Secondly, the double layer capacitance (C_{dl}) value declines with enhancing the inhibitor concentration due to the reduction in local dielectric constant and/or enhance the density of electrical double layer, which implies that used oxadiazole derivatives (low dielectric constant) function *via* adsorption at metal/solution interface by the action of displacement of pre-adsorbed water molecules (high dielectric constant) from the metal surface [58,59].

The values of C_{dl} were computed through the frequency value at which the imaginary component of the impedance is ($-Z_{max}$) maximal and R_{ct} value by using eqn. 8 [60]:

TABLE-3
CALCULATED THERMODYNAMIC ADSORPTION PARAMETERS ON CORROSION OF MILD STEEL IN 1.0 M HCl IN THE EXISTENCE OF NUMEROUS CONCENTRATIONS OF APOT AND MPOT AT VARYING TEMPERATURES FOR AN IMMERSION PERIODS OF 12 h

Temperature (K)	APOT				MPOT			
	R^2	K_{ads} (g L^{-1})	Slope	ΔG° (kJ/mol)	R^2	K_{ads} (g L^{-1})	Slope	ΔG° (kJ/mol)
298	0.996	17.95	1.08	-24.27	0.994	19.82	1.10	-24.51
308	0.990	16.01	1.15	-24.79	0.993	18.24	1.17	-25.12
318	0.990	13.52	1.20	-25.15	0.988	16.34	1.20	-25.65

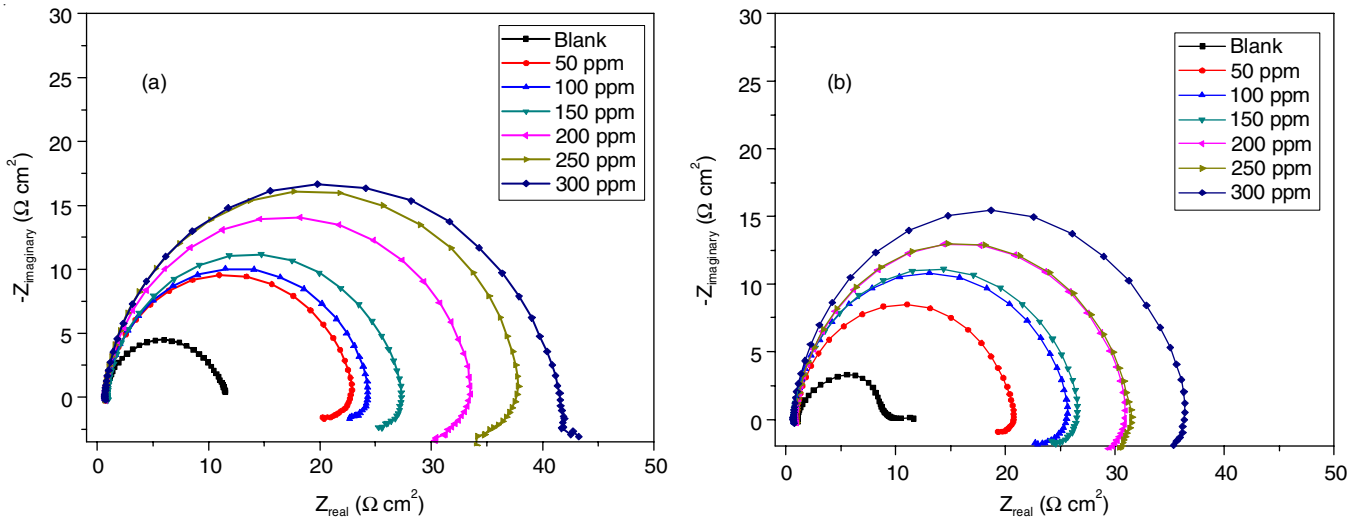

Fig. 8. Nyquist curves for mild steel in 1.0 M HCl solution in presence of numerous concentrations (a) APOT, (b) MPOT as corrosion inhibitors at 298 K

TABLE-4
ELECTROCHEMICAL IMPEDANCE CRITERIONS AND THEIR EQUIVALENT INHIBITION EFFICIENCY FOR MILD STEEL IN 1.0 M HCl IN PRESENCE OF NUMEROUS CONCENTRATIONS OF APOT AND MPOT AT 298 K

Conc. (ppm)	APOT						MPOT					
	R_{ct} (Ω cm²)	CPE/$Y_0 \times 10^6$ (S cm^{-2} S^{n2})	n	χ^2	C_{dl} (μF cm^{-2})	η_{eis} (%)	R_{ct} (Ω cm²)	CPE/$Y_0 \times 10^6$ (S cm^{-2} S^{n2})	n	χ^2	C_{dl} (μF cm^{-2})	η_{eis} (%)
Blank	10.77	165.6	0.997	0.949	128.40	–	10.60	167.3	0.990	0.929	130.46	–
50	22.32	141.3	0.983	0.792	61.96	51.74	20.10	149.1	0.949	0.868	68.80	47.26
100	24.30	134.8	0.899	1.001	56.91	55.67	24.29	137.3	0.888	0.976	56.93	56.36
150	27.10	127.5	0.882	0.922	51.03	60.25	26.30	129.8	0.908	0.990	52.58	59.69
200	33.27	116.0	0.943	0.870	41.56	67.62	30.10	122.4	0.986	0.896	45.94	64.78
250	37.37	101.3	0.962	0.775	37.00	71.18	31.15	108.6	0.882	0.835	44.39	65.97
300	43.30	90.2	0.879	0.664	31.93	75.12	36.32	97.1	0.896	0.660	38.07	70.81

$$C_{dl} = \frac{1}{2\pi f_{max}} \times \frac{1}{R_{ct}} \quad (8)$$

where, f_{max} is the value of frequency at highest point of semicircle of Z_{real} axis and R_{ct} is charge transfer resistance.

To determine the percentage inhibition efficiency (η_{eis}%), the R_{ct} value was computed by the following relation (eqn. 9):

$$\eta_{eis}\% = \frac{R_{ct(inh)} - R_{ct}}{R_{ct(inh)}} \times 100 \quad (9)$$

where, R_{ct} and $R_{ct\,(inh)}$ depicts the charge transfer resistance in without and with of various concentrations of both inhibitor molecules, respectively.

Fig. 9a-b show the bode modules curve of log Z *vs.* log f and Fig. 9c-d depict the bode phase of phase angle *vs.* log f for corrosion of mild steel surface in 1.0 M HCl with presence of both inhibitors at 298 K. Fig. 9a-b reveals that Bode modulus (impedance value) increased with increase inhibitors concentrations in 1.0 M HCl, which results in the retardation of corrosion value at the mild steel surface [61]. In Fig. 9c-d, it is clear that the phase angle value enhanced with the increasing concentration, which indicates that the metal/solution interface display the capacitive action on mild steel surface [62]. The maximum phase angle value were found at the intermediate frequencies and the maximum value expresses that the barrier protective film of both inhibitors formed on mild steel surface which protect against corrosion process.

Besides, Fig. 9e exposed an equivalent circuit diagram, which perform to investigate the electrochemical impedance statistics and different impedance parameters linked to fitted with circuit diagram like constant phase element (CPE), chi square (χ^2) and n values. The diagram contains a solution resistance (R_s), constant phase element (CPE) and charge transfer resistance (R_{ct}) where, CPE constituent is working to determine the clue related to the arrangement of double-layer at electrode (metal)/electrolyte (solution) interface. Also, n value identical to -1, 0, 0.5 and 1 as connected with inductance, resistance, Warburg impedance and capacitance, respectively [63]. The CPE impedance was inspected by using eqn. 10 [64]:

$$Z_{CPE} = \left(\frac{1}{Y^0}\right)[(j\omega)_n]^{-1} \quad (10)$$

where, Y^0 is CPE constant, ω represents angular frequency and j denotes imaginary number respectively.

In present studies, maximal corrosion inhibition efficiency values were observed 75.12% for APOT and 70.81% for MPOT at 300 ppm in 1.0 M HCl. Hence, the above impedance concluded that an inhibition efficiency of each inhibitor is nearly identical with the data obtained from weight loss analysis.

Potentiodynamic polarization measurement: The plots of potentiodynamic polarization for mild steel surface in 1.0

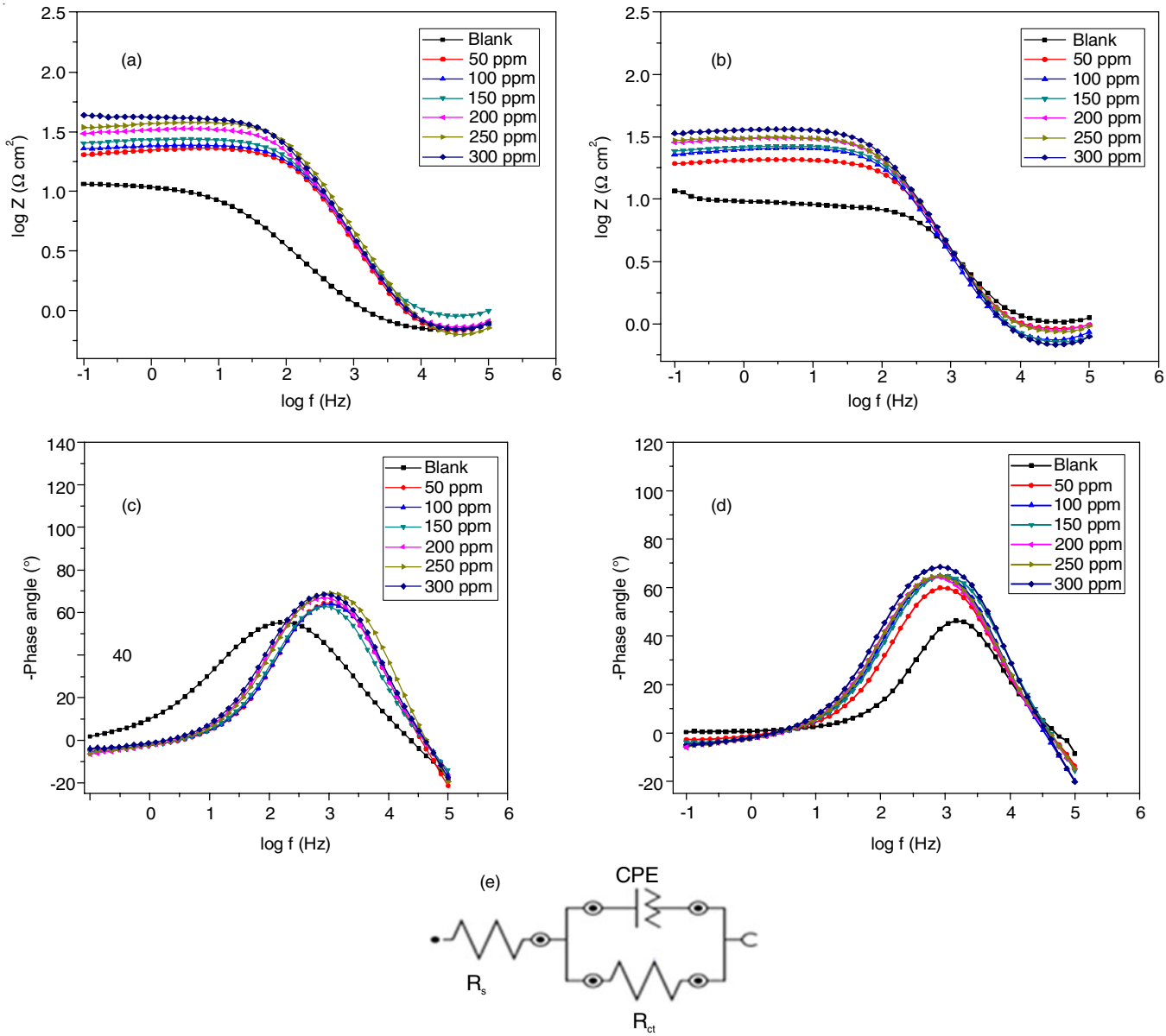

Fig. 9. Bode modules plots of (a) APOT (b) MPOT and phase angle plots of (c) APOT and (d) MPOT respectively, (e) an equivalent circuit diagram recommended to fitting the EIS data

M HCl with various concentrations of inhibitors are displayed in Fig. 10. It is observed that both cathodic as well as anodic reactions were inhibited, which implied that both inhibitors diminishes the anodic metal disintegration and in addition to retarded the rate of cathodic hydrogen evolution reaction [65], which further explain that there is reduction of corrosion rate. The reason is attributed that both inhibitors compounds adsorbed on to mild steel surface through π-electrons and free electron pair from hetroatoms [54]. Hence, both studied inhibitors categorized as mixed type corrosion inhibitors.

Various potentiodynamic polarization parameters like the value of corrosion current densities (I_{corr}) and corrosion potential (E_{corr}) are acquired from the extrapolations of Tafel area of anodic and cathodic curves, cathodic (β_c) and anodic (β_a). The Tafel constant value obtained through slopes of linear region of polarization curves and the percentage corrosion inhibition efficiency are reported in Table-5.

From Table-5, it is certainly noticed that the I_{corr} value is lower in the inhibited solution than uninhibited solution and decrease with increasing the concentration of each inhibitors which is likewise dominant in increasing the percentage inhibition efficiency. The enhanced corrosion percentage inhibition efficiency was caused due to the blocking of the active places through forming of inhibitive coating of corrosion inhibitor which adsorbed on the surface of mild steel. Besides this, Tafel constant β_c and β_a values are slightly changed in presence of both studied inhibitors concentration, which recommended that on adding the inhibitor concentration decreases the cathodic hydrogen evolution including anodic dissolution of mild steel without changing the reaction mechanism [66].

The values of β_c and β_a Tafel constant and polarization resistance (R_p) were also employed to determine the corrosion current density (I_{corr}). Hence I_{corr} value was determined by utilizing Stern-Geary equation (eqn. 11):

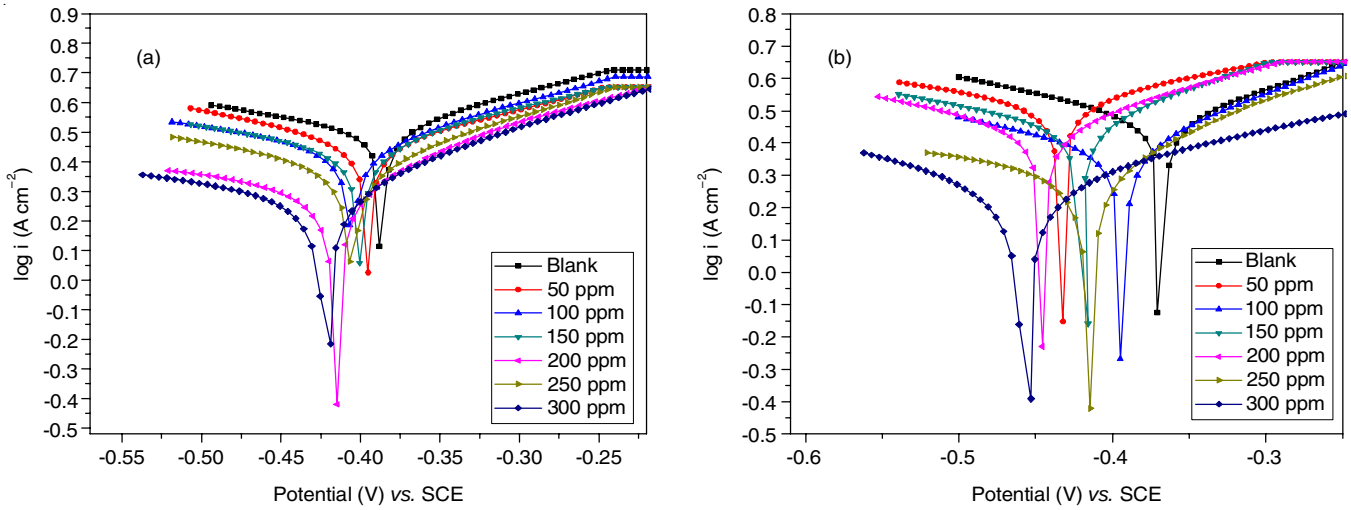

Fig. 10. Potentiodynamic polarization plots for MS in 1.0 M HCl in presence of numerous concentrations of (a) APOT and (b) for MPOT at the 298 K

TABLE-5
POTENTIODYNAMIC POLARIZATION MEASUREMENTS FOR MILD STEEL IN 1.0 M HCl IN EXISTENCE OF NUMEROUS CONCENTRATIONS OF APOT AND MPOT AT 298 K

Conc. (ppm)	APOT						MPOT					
	β_a (mV dec^{-1})	β_c (mV dec^{-1})	R_p (μ cm^2)	$-E_{corr}$ (mV *vs.* SCE)	I_{corr} (μA cm^{-2})	η_{pol} (%)	β_a (mV dec^{-1})	β_c (mV dec^{-1})	R_p (μ cm^2)	$-E_{corr}$ (mV *vs.* SCE)	I_{corr} (μA cm^{-2})	η_{pol} (%)
Blank	362	139	13.96	423.27	3.12	–	381	163	14.69	419.35	3.37	–
50	307	128	23.78	449.43	1.64	47.43	290	147	22.14	442.56	1.91	43.32
100	279	152	28.15	438.72	1.51	51.60	316	142	25.57	454.92	1.66	51.24
150	296	134	32.39	464.90	1.23	60.57	273	155	29.76	431.48	1.44	57.27
200	241	129	35.66	479.03	1.02	67.30	198	173	32.04	467.19	1.25	62.90
250	229	120	37.13	462.18	0.92	70.51	218	138	33.62	474.85	1.09	67.65
300	205	137	41.56	496.22	0.85	72.75	258	119	36.01	488.44	0.98	70.91

$$I_{corr} = \frac{\beta_a \times \beta_c}{2.303(\beta_a + \beta_c)} \times \frac{1}{R_p} \quad (11)$$

where, β_c and β_a are the cathodic and anodic Tafel constant, respectively; and R_p is the polarization resistance.

The polarization percentage corrosion inhibition efficiency was calculated using I_{corr} value *via* consequent equation (eqn. 12):

$$\eta_{pol}\% = \left(1 - \frac{I_{corr^i}}{I_{corr^o}}\right) \times 100 \quad (12)$$

where, I_{corr^o} and I_{corr^i} are the corrosion current densities of mild steel with absence and presence of inhibitors concentration in 1.0 M HCl.

Table-5 also indicate that the shift of corrosion potential (E_{corr}) at different concentrations of both inhibitors does not follow an exact orders. After all, if the shift of corrosion potential (E_{corr}) with addition of inhibitors concentrations is above 85 mV, then the corrosion inhibitor may be categorized as cathodic or anodic nature of corrosion inhibitor and if the shift of corrosion potential (E_{corr}) is lower than 85 mV, then it is identified as mixed type behaviour of corrosion inhibitor which can affects combined anodic metal disintegration and cathodic hydrogen evolution reactions [67-69]. In present investigations, the maximum change of corrosion potential value between uninhibited solution and maximum concentration of inhibitors containing solution is 73 mV for APOT and 69 mV for MPOT, which confirmed that these two studied inhibitors molecules are mixed type for mild steel in 1.0 M HCl.

Moreover, the order of both oxadiazole derivatives that related to corrosion inhibition efficiency at 300 ppm in 1.0 M HCl solution is APOT > MPOT, which might be likely as presence of extra N-heteroatoms in the structure of APOT. The maximal corrosion inhibition efficiency ($\eta_{pol\%}$) related to I_{corr} value was considered to be 72.75 for APOT and 70.91 for MPOT at 300 ppm. The obtained corrosion inhibition efficiencies value though impedance and polarization experiments are lower in respect to that obtained by the weight loss measurement. This difference can be illustrated by the fact that in electrochemical analysis, there is the instantaneous corrosion current measured. But regarding the weight loss method, inhibition efficiency is calculated after immersion periods of 12 h. Thus, it exhibit that an increase of immersion time periods, the adsorption ability of inhibitor compound on to surface of mild steel was found to be strong.

Surface study

SEM analysis: The surface characterization of mild steel polished surface and subsequently weight loss experiment

without and with various concentrations of APOT and MPOT in 1.0 M HCl immersed for 12 h at 298 K are shown in Fig. 11a-d. For both inhibitors, the surface of mild steel specimen were substantially protected which can be associated to the development of inhibitive coating of inhibitors on mild steel surface Fig. 11a display the morphology of freshly polished mild steel surface which seems to be clear, uniform and smooth. In the solution of 1.0 M HCl, Fig. 11b displays the surface of mild steel is highly corroded, broken, damaged and rough as a result of corrosion of mild steel and the disintegration of metal surface in 1.0 M HCl. However, at 300 ppm, both inhibitors added to the acidic solution, the morphology of mild steel surface less corroded and becomes almost smooth surface as shown in Fig. 11c-d [70]. As a consequence, the results recommended that there is a formation of inhibitive layer on mild steel surface with the addition of 300 ppm corrosion inhibitors in 1.0 M HCl, which may inhibit the surface of mild steel from a corrosive media.

EDX analysis: EDX spectroscopy may be accomplished to conclude the elemental composition of mild steel specimens in 1.0 M HCl in the presence of 300 ppm APOT and MPOT for 12 h immersion at 298 K. The X-rays which have enough energy to escape the metal surface could be identified, appearing in a spectrum with peak of the characteristic energies for the components are presented in Fig. 12a for 1.0 M HCl in absence of inhibitor, (b) with 300 ppm concentration of APOT and (c) for MPOT.

Moreover, atomic percentage of elements found in EDX analysis for mild steel in 1.0 M HCl is 47.47% O, 29.49% Fe and 14.53% C, *etc*. These results for uninhibited solution for mild steel surface imply that the corrosion of mild steel surface is due to a higher percentage of oxygen, which forms the iron oxide film on the surface. The percentage elements composition

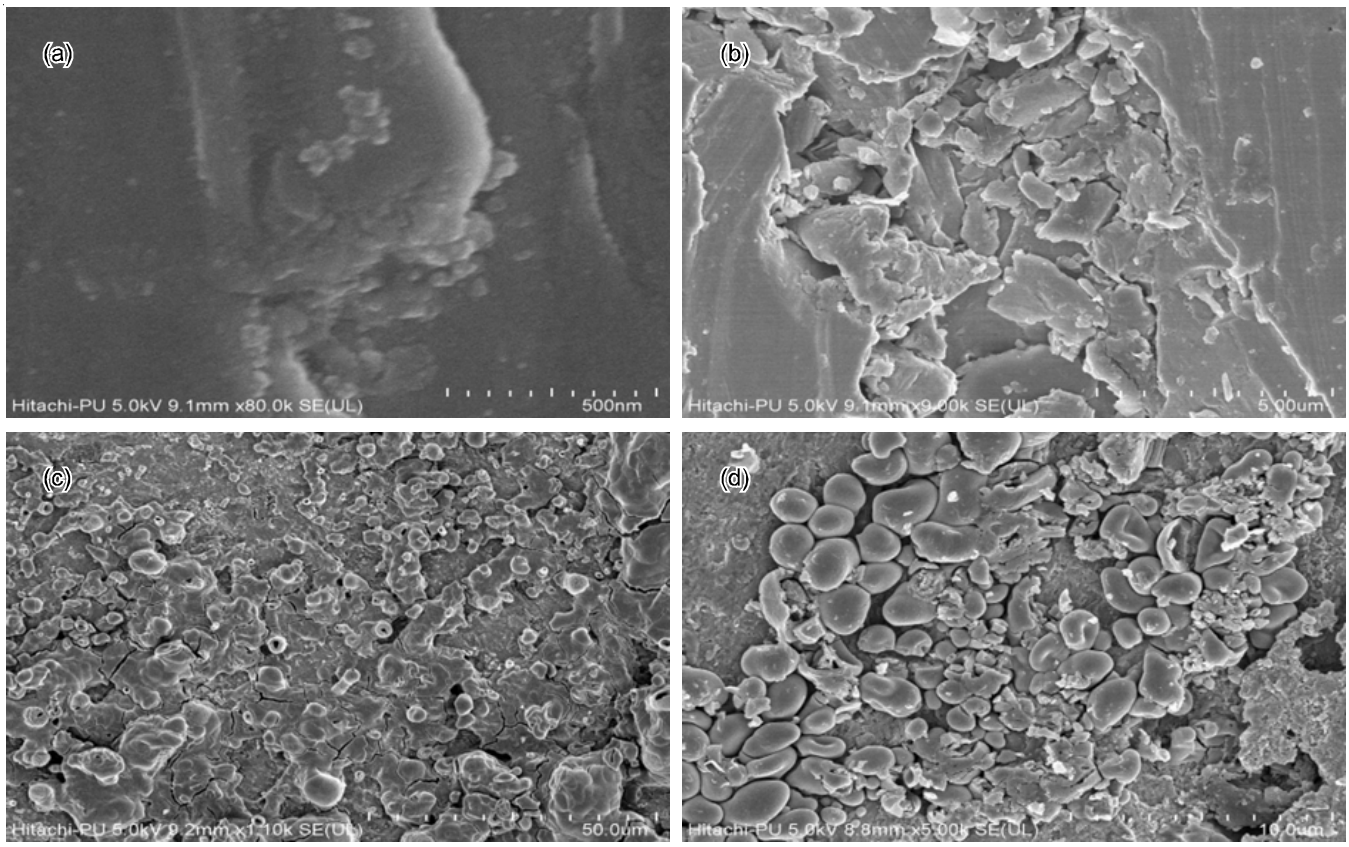

Fig. 11. SEM illustration for mild steel surface (a) polished surface of mild steel (b) immersed in 1.0 M HCl solution (b) with 300 ppm concentration of (c) APOT and (d) MPOT at 298 K

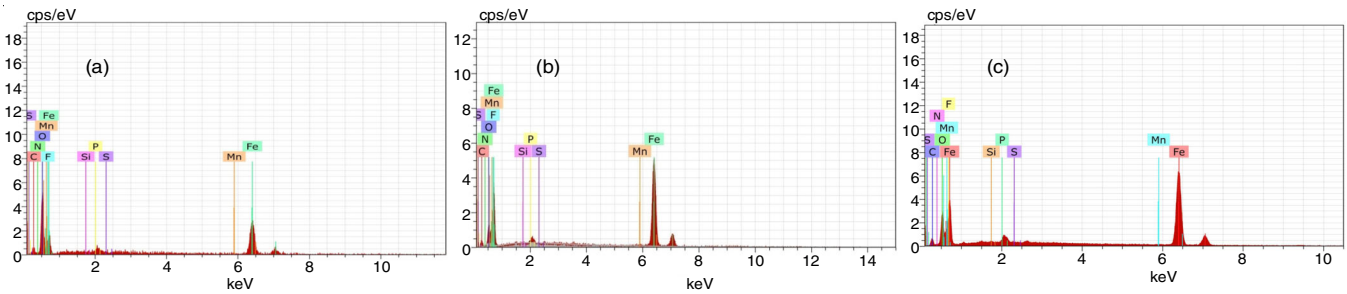

Fig. 12. EDX spectrum for mild steel surface (a) 1.0 M HCl solution (a) with 300 ppm concentration of (b) APOT and (c) MPOT at 298 K for an immersion period of 12 h

for 300 ppm APOT, 39.19% O, 0.56% N, 0.06% S and 48.57% Fe and for MPOT, 40.12% O, 0.51% N, 0.04% S and 42.17% Fe indicates that the peak of oxygen in both inhibitors significantly decreased, which concludes that there is decrease in a density of corrosion active centers and also confirmed the existence of used inhibitors concentration in 1.0 M HCl. Further, all these experimental data explains that the presence of inhibitors formed a protective layer through strong adsorption on mild steel surface to protect the surface against corrosion.

Conclusion

Two new oxadiazole derivatives [5-(4-aminophenyl)-1,3,4-oxadiazole-2-thiol (APOT) and 5-(4-methylphenyl)-1,3,4-oxadiazole-2-thiol (MPOT)] were investigated as new corrosion inhibitors on mild steel surface in 1.0 M HCl using weight loss and electrochemical techniques. Through, the weight loss estimation it tends to be seen that on enhancing the inhibitor concentration in acidic solution, the inhibition efficiency enhance but corrosion rate diminish. Potentiodynamic polarization plots signified that the inhibitor behaved as mixed type by controlling the hydrogen evolution and metal disintegration reaction. Whereas, electrochemical impedance results exhibit that the charge transfer resistance enhance but double layer capacitance diminishes with the increasing inhibitor concentration. Adsorption phenomenon obeys the Langmuir adsorption isotherm. Further, an activation energy of both inhibitors was greater for inhibited solution than uninhibited 1.0 M HCl. The positive enthalpy of activation value explains the destruction of mild steel is endothermic in nature and the entropy of activation indicates the decline in the rate of metal dissolution. The thermodynamic parameters of adsorption process imply the adsorption behaviour was spontaneous and physical in nature. The SEM and EDX analysis of mild steel surface exposed the evolution of inhibitive film of APOT and MPOT inhibitors on surface of mild steel. All the results acquired from different techniques are in reasonable agreement.

CONFLICT OF INTEREST

The authors declare that there is no conflict of interests regarding the publication of this article.

REFERENCES

1. S. Saravanamoorthy and S. Velmathi, *Prog. Org. Coat.*, **76**, 1527 (2013); https://doi.org/10.1016/j.porgcoat.2013.06.003
2. K. Zhang, B. Xu, W. Yang, X. Yin, Y. Liu and Y. Chen, *Corros. Sci.*, **90**, 284 (2015); https://doi.org/10.1016/j.corsci.2014.10.032
3. S.M. Shaban, I. Aiad, M.M. El-Sukkary, E.A. Soliman and M.Y. El-Awady, *J. Mol. Liq.*, **203**, 20 (2015); https://doi.org/10.1016/j.molliq.2014.12.033
4. A.A. Farag and T.A. Ali, *J. Ind. Eng. Chem.*, **21**, 627 (2015); https://doi.org/10.1016/j.jiec.2014.03.030
5. D. Dwivedi, K. Lepková and T. Becker, *RSC Adv.*, **7**, 4580 (2017); https://doi.org/10.1039/C6RA25094G
6. A.K. Singh and M.A. Quraishi, *Corros. Sci.*, **52**, 1529 (2010); https://doi.org/10.1016/j.corsci.2009.12.011
7. S.S. de Assunção Araújo Pereira, M.M. Pêgas, T.L. Fernández, M. Magalhães, T.G. Schöntag, D.C. Lago, L.F. de Senna and E. D'Elia, *Corros. Sci.*, **65**, 360 (2012); https://doi.org/10.1016/j.corsci.2012.08.038
8. A.K. Satapathy, G. Gunasekaran, S.C. Sahoo, K. Amit and P.V. Rodrigues, *Corros. Sci.*, **51**, 2848 (2009); https://doi.org/10.1016/j.corsci.2009.08.016
9. J.C. da Rocha, J.A. da Cunha Ponciano Gomes and E. D'Elia, *Corros. Sci.*, **52**, 2341 (2010); https://doi.org/10.1016/j.corsci.2010.03.033
10. S.W. Dean Jr. and R. Derby, *Mater. Perform.*, **20**, 47 (1981).
11. O.L. Riggs Jr., Corrosion Inhibitors, C.C. Nathan, Houston, TX, Ed.: 2 (1973).
12. S.M.A. Hosseini and A. Azimi, *Corros. Sci.*, **51**, 728 (2009); https://doi.org/10.1016/j.corsci.2008.11.019
13. F. Bentiss, C. Jama, B. Mernari, H.E. Attari, L.E. Kadi, M. Lebrini, M. Traisnel and M. Lagrenée, *Corros. Sci.*, **51**, 1628 (2009); https://doi.org/10.1016/j.corsci.2009.04.009
14. P. Lowmunkhong, D. Ungthararak and P. Sutthivaiyakit, *Corros. Sci.*, **52**, 30 (2010); https://doi.org/10.1016/j.corsci.2009.08.039
15. A.A. Rahim, E. Rocca, J. Steinmetz, M.J. Kassim, R. Adnan and M. Sani Ibrahim, *Corros. Sci.*, **49**, 402 (2007); https://doi.org/10.1016/j.corsci.2006.04.013
16. W. Li, Q. He, C. Pei and B. Hou, *Electrochim. Acta*, **52**, 6386 (2007); https://doi.org/10.1016/j.electacta.2007.04.077
17. L.L. Liao, S. Mo, H.Q. Luo, Y.J. Feng, H.Y. Yin and N.B. Li, *Corros. Sci.*, **124**, 167 (2017); https://doi.org/10.1016/j.corsci.2017.05.020
18. M. Muralisankar, R. Sreedharan, S. Sujith, N.S.P. Bhuvanesh and A. Sreekanth, *J. Alloys Compd.*, **695**, 171 (2017); https://doi.org/10.1016/j.jallcom.2016.10.173
19. A. Ghazoui, N. Benchat, F. El-Hajjaji, M. Taleb, Z. Rais, R. Saddik, A. Elaatiaoui and B. Hammouti, *J. Alloys Compd.*, **693**, 510 (2017); https://doi.org/10.1016/j.jallcom.2016.09.191
20. M. Lebrini, F. Bentiss, H. Vezin and M. Lagrenee, *Appl. Surf. Sci.*, **252**, 950 (2005); https://doi.org/10.1016/j.apsusc.2005.01.160
21. M. Bouklah, B. Hammouti, M. Lagrenee and F. Bentiss, *Corros. Sci.*, **48**, 2831 (2006); https://doi.org/10.1016/j.corsci.2005.08.019
22. F. Bentiss, M. Traisnel, H. Vezin, H.F. Hildebrand and M. Lagrenée, *Corros. Sci.*, **46**, 2781 (2004); https://doi.org/10.1016/j.corsci.2004.04.001
23. L. Herrag, A. Chetouani, S. Elkadiri, B. Hammouti and A. Aouniti, *Electrochim. Acta*, **26**, 211 (2007); https://doi.org/10.4152/pea.200802211
24. A. El-Ouafi, B. Hammouti, H. Oudda, S. Kertit, R. Touzani and A. Ramdani, *Anti-Corros. Methods Mater.*, **49**, 199 (2002); https://doi.org/10.1108/00035590210426463
25. M.A. Quraishi and R. Sardar, *Corrosion*, **58**, 748 (2002); https://doi.org/10.5006/1.3277657
26. L. Wang, M.J. Zhu, F.C. Yang and C.-W. Gao, *Int. J. Corros.*, **2012**, 573964 (2012); https://doi.org/10.1155/2012/573964
27. P. Liu, X. Fang, Y. Tang, C. Sun, C. Yao, *Mater. Sci. Appl.*, **2**, 1268 (2011); https://doi.org/10.4236/msa.2011.29171
28. F. Chaouket, B. Hammouti, S. Kertit and K.E. Kacemi, *Bull. Electrochem.*, **17**, 311 (2001).
29. M.H. Wahdan and G.K. Gomma, *Mater. Chem. Phys.*, **47**, 176 (1997); https://doi.org/10.1016/S0254-0584(97)80048-X
30. F. Bentiss, M. Traisnel, H. Vezin and M. Lagrenee, *Corros. Sci.*, **45**, 371 (2003); https://doi.org/10.1016/S0010-938X(02)00102-6
31. M. Lagrenee, B. Mernari, N. Chaibi, M. Traisnel, H. Vezin and F. Bentiss, *Corros. Sci.*, **43**, 951 (2001); https://doi.org/10.1016/S0010-938X(00)00076-7
32. A.F. Emmanuel, Ph.D. Thesis, Ahmadu Bello University, Zaria, Nigeria (2011).
33. V. Kalia, P. Kumar, S. Kumar, P. Pahuja, G. Jhaa, S. Lata and H. Dahiya, *J. Mol. Liq.*, **313**, 113601 (2020); https://doi.org/10.1016/j.molliq.2020.113601
34. I.B. Obot, N.O. Obi-Egbedi and S.A. Umoren, *Corros. Sci.*, **51**, 1868 (2009); https://doi.org/10.1016/j.corsci.2009.05.017

35. T. Horvath, E. Kalman, G. Kutsan and A. Rauscher, *Br. Corros. J.*, **29**, 215 (1994); https://doi.org/10.1179/000705994798267683
36. G. Gunasekaran, R. Natarajan, V.S. Muralidharan, N. Palaniswamy and B.V. Apparao, *Indian J. Chem. Technol.*, **5**, 91 (1998).
37. G. Gunasekaran, R. Natarajan, V.S. Muralidharan, N. Palaniswamy and B.V. Apparao, *Proc. Ind. Acad. Sci. Chem. Sci.*, **108**, 399 (1996).
38. L. Wang, G.-J. Yin and J.-G. Yin, *Corros. Sci.*, **43**, 1197 (2001); https://doi.org/10.1016/S0010-938X(00)00138-4
39. I. Ahamad and M.A. Quraishi, *Corros. Sci.*, **52**, 651 (2010); https://doi.org/10.1016/j.corsci.2009.10.012
40. C. Verma, M.A. Quraishi and A. Singh, *J. Taiwan Inst. Chem. Eng.*, **49**, 229 (2015); https://doi.org/10.1016/j.jtice.2014.11.029
41. E.E. Oguzie, C. Unaegbu, C.N. Ogukwe, B.N. Okolue and A.I. Onuchukwu, *Mater. Chem. Phys.*, **84**, 363 (2004); https://doi.org/10.1016/j.matchemphys.2003.11.027
42. Y. Abboud, A. Abourriche, T. Saffaj, M. Berrada, M. Charrouf, A. Bennamara and H. Hannache, *Desalination*, **237**, 175 (2009); https://doi.org/10.1016/j.desal.2007.12.031
43. O. Sikemi, O.A. Kolawole and S. Banjo, *Manila J. Sci.*, **10**, 44 (2017).
44. C. Verma, M.A. Quraishi and A. Singh, *J. Mol. Liq.*, **212**, 804 (2015); https://doi.org/10.1016/j.molliq.2015.10.026
45. M.R. Laamari, J. Benzakour, F. Berrekhis, A. Derja and D. Villemin, *Arab. J. Chem.*, **9**, S245 (2016); https://doi.org/10.1016/j.arabjc.2011.03.018
46. P. Preethi Kumari, P. Shetty and S.A. Rao, *Arab. J. Chem.*, **10**, 653 (2017); https://doi.org/10.1016/j.arabjc.2014.09.005
47. G. Moretti, F. Guidi and F. Fabris, *Corros. Sci.*, **76**, 206 (2013); https://doi.org/10.1016/j.corsci.2013.06.044
48. R. Solmaz, E.A. Sahin, A. Doner and G. Kardas, *Corros. Sci.*, **53**, 3231 (2011); https://doi.org/10.1016/j.corsci.2011.05.067
49. K.K. Anupama, K. Ramya and A. Joseph, *J. Mol. Liq.*, **216**, 146 (2016); https://doi.org/10.1016/j.molliq.2016.01.019
50. N.A. Negm, F.M. Ghuiba and S.M. Tawk, *Corros. Sci.*, **53**, 3566 (2011); https://doi.org/10.1016/j.corsci.2011.06.029
51. S.A. Umoren, I.B. Obot, A. Madhankumar and Z.M. Gasem, *Carbohydr. Polym.*, **124**, 280 (2015); https://doi.org/10.1016/j.carbpol.2015.02.036
52. A.A. Nazeer, K. Shalabi, A.S. Fouda, *Res. Chem. Intermed.*, **41**, 4833 (2015); https://doi.org/10.1007/s11164-014-1570-4
53. J. Villanueva, L. Trino, J. Thomas, D. Bijukumar, D. Royhman, M.M. Stack and M.T. Mathew, *J. Biol. Tribo-Corros.*, **3**, 1 (2017); https://doi.org/10.1007/s40735-016-0060-1
54. M.A. Amin, S.S. Abd El-Rehim, E.E.F. El-Sherbini and R.S. Bayoumi, *Electrochim. Acta*, **52**, 3588 (2007); https://doi.org/10.1016/j.electacta.2006.10.019
55. W. Li, Q. He, S. Zhang, C. Pei and B. Hou, *J. Appl. Electrochem.*, **38**, 289 (2008); https://doi.org/10.1007/s10800-007-9437-7
56. R. Yildiz, T. Dogan and I. Dehri, *Corros. Sci.*, **85**, 215 (2014); https://doi.org/10.1016/j.corsci.2014.04.017
57. F. Bentiss, M. Traisnel and M. Lagrenee, *Corros. Sci.*, **42**, 127 (2000); https://doi.org/10.1016/S0010-938X(99)00049-9
58. M.N. El-Haddad, *Int. J. Biol. Macromol.*, **55**, 142 (2013); https://doi.org/10.1016/j.ijbiomac.2012.12.044
59. H. Bouammali, C. Jama, K. Bekkouch, A. Aouniti, B. Hammouti and F. Bentiss, *J. Ind. Eng. Chem.*, **26**, 270 (2015); https://doi.org/10.1016/j.jiec.2014.11.039
60. D. Daoud, T. Douadi, S. Issaadi and S. Chafaa, *Corros. Sci.*, **79**, 50 (2014); https://doi.org/10.1016/j.corsci.2013.10.025
61. A. Singh, K.R. Ansari, J. Haque, P. Dohare, H. Lgaz, R. Salghi and M.A. Quraishi, *J. Taiwan Inst. Chem. Eng.*, **82**, 233 (2018); https://doi.org/10.1016/j.jtice.2017.09.021
62. K.R. Ansari, D.K. Yadav, E.E. Ebenso and M.A. Quraishi, *Int. J. Electrochem. Sci.*, **7**, 4780 (2012).
63. M.A. Hegazy, *Corros. Sci.*, **51**, 2610 (2009); https://doi.org/10.1016/j.corsci.2009.06.046
64. R. Kumar, S. Chahal, S. Kumar, S. Lata, H. Lgaz, R. Salghi and S. Jodeh, *J. Mol. Liq.*, **243**, 439 (2017); https://doi.org/10.1016/j.molliq.2017.08.048
65. A.S. Fouda, Y.A. Elewady and H.K. Abd El-Aziz, *J. Chem. Sci. Technol.*, **1**, 45 (2012).
66. K.C.D.B. Yadav, M.A. Maiti and M.A. Quraishi, *Corros. Sci.*, **52**, 3586 (2010); https://doi.org/10.1016/j.corsci.2010.06.030
67. W. Al Zoubi, S.G. Mohamed, A.A.S. Al-Hamdani, A.P. Mahendradhany and Y.G. Ko, *RSC Adv.*, **8**, 23294 (2018); https://doi.org/10.1039/C8RA01890A
68. E. Ituen, O. Akaranta, A. James and S. Sun, *Sustain. Mater. Technol.*, **11**, 12 (2017); https://doi.org/10.1016/j.susmat.2016.12.001
69. N. Hassan, S.M. Ali, A. Ebrahim and H. El-Adawi, *Mater. Res. Express*, **6**, 0865c7 (2019); https://doi.org/10.1088/2053-1591/ab2376
70. A. Singh, Y. Lin, E. Ebenso and W. Liu, *Int. J. Electrochem. Sci.*, **9**, 5585 (2014).